

Chapter 4. Prototypes and Results

This research was considered as very ambitious and the results not guaranteed when it was first started in fall 1996. The main objective was to produce an accurate model of a distributed active-passive absorber and possibly, in the future, realize a prototype. The design of a prototype was a challenge since nothing yet existed like it. Several ideas were first tried using piezoelectric rubber as the active stiffness layer but the stiffness of the system was always too high for use as part of an absorber with useable resonant frequency. The idea of using polyvinylidene fluoride (PVDF) film as the active stiffness layer film comes from the research on smart skins performed in the Vibration and Acoustics Laboratories (VAL) at Virginia Tech [22]. The very first prototype built using PVDF demonstrated the low stiffness of the absorber, the second prototype proved its efficiency on a real structure and the third was the first complete active-passive distributed absorber.

4.1 Distributed absorber with constant mass distribution

4.1.1 Design

A vibration absorber is constituted of two elements: a spring element and a mass element. The point absorber presented in Chapter 2, figure 2.4 and 2.5, is based on this principle. The main element is the active spring element. It is a hybrid system with piezoelectric discs requiring precision manufacturing. The design of a distributed absorber implies the use of a distributed spring and distributed mass as was presented figure 2.11. The main design effort is focused on the distributed spring element. Locally, the distributed absorber must have the same resonance frequency as the point absorber presented earlier.

The mass allocated locally is just a fraction of the total mass and for this reason the local stiffness has to be a fraction of the global stiffness. The creation of an active elastic layer with very low stiffness is the main design challenge. For this reason, the mass distribution was not a concern at first. A distributed active vibration absorber (DAVA) with constant mass distribution was thus first investigated.

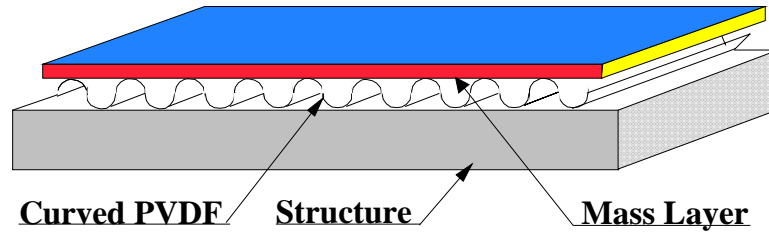


Figure 4.1: DAVA prototype design

Figure 4.2 presents the basic design of the DAVA. This design follows exactly the two layer design concept discussed previously. The first layer is an elastic layer with low stiffness that can be electrically activated. It is made of polyvinylidene fluoride (PVDF) of thickness 10 μm . The second layer is a distributed mass, which has a constant thickness. This layer is made out of a thin sheet of lead. This absorber is designed to weight 10% of the structure supporting it. The thickness of the lead layer depends directly on the weight per unit area of the main structure. For a steel beam or plate, the maximum thickness of a uniform lead layer can be easily calculated, neglecting the weight of the elastic layer.

$$\frac{h_m}{h_b} = \frac{\rho_b}{\rho_m} * 10\% = \frac{7800}{11300} * 10\% = 7\% \quad (4.1)$$

For a steel beam of 6.35 mm, the maximum thickness of the lead mass layer of a DAVA is 0.44mm. This is assuming that the DAVA covers the all surface of the beam. With this weight limitation, an elastic layer with a very low stiffness is a necessity. This is especially true for the control of low frequencies. For example, with a 1mm thick mass

layer (made of lead), the stiffness of a 2 mm thick elastic layer has to be $9e+5$ N/m in order to obtain a resonance frequency at 1000 Hz.



Figure 4.2: Prototype #1

Figure 4.1 presents the first prototype that validated the elastic layer concept described earlier. A corrugated piece of plastic is glued together with a thin sheet of lead. This early distributed absorber is positioned on a rigid aluminum base and partly validates the mechanical design. The experiments and properties of this absorber are discussed in Section 4.1.3. The plastic material PVDF used for the elastic layer is a piezoelectric material. This piezoelectric sheet will mechanically shrink and expand under the influence of an electric field. On each side of the PVDF two thin layers of silver act as electrodes. If a voltage is applied between these electrodes, an electric field is created within the material. For more information about piezoelectric actuators and the use of PVDF, the reader is referred to the text “Active Control of Vibration” [6]. In the DAVA design, the PVDF film is curved to increase the amplitude of motion and decrease the stiffness of the system. The PVDF film is glued with epoxy on two thin sheets of plastic at the points shown in Figure 4.3 where it contacts the beam and lead layer so that it does not lose its shape with time by expanding in the axial direction.

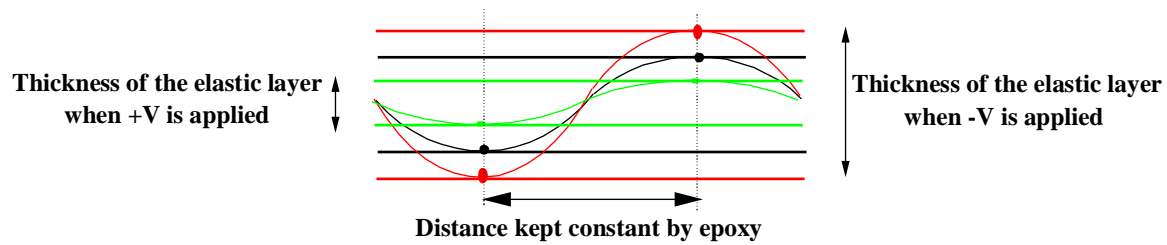


Figure 4.3: Motion under electrical excitation

Figure 4.3 presents the motion of the elastic layer under electrical excitation. The black line is the layer at rest, the red line is the layer when $-V$ is applied and the green line is the layer when $+V$ is applied. The two sheets of plastic on both side of the layer prevent any axial motion. When a voltage is applied, the length of the PVDF film changes. As a consequence, the distance between the two planes on each side of the absorber is also changed. The design of the absorber transforms the in-plane motion of the PVDF into the out-of-plane motion of the elastic layer.

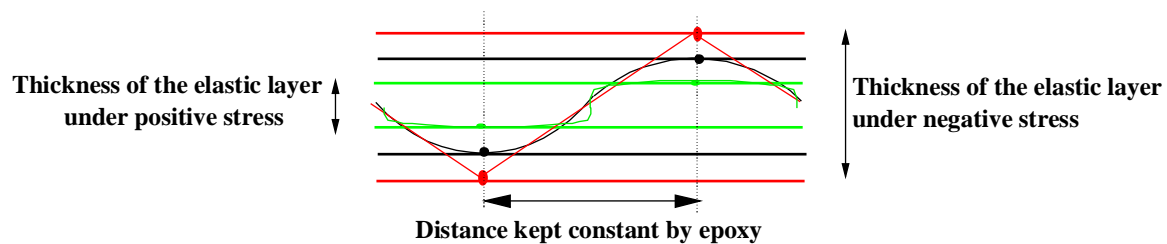


Figure 4.4: Motion under mechanical excitation

Figure 4.4 presents the motion of the elastic layer under mechanical excitation. The black line is the layer at rest, the red line is the layer when a negative load is applied and the green line is the layer when a positive load is applied. When the absorber is constrained by mechanical forces, the length of the PVDF does not change (stiffness c_{11} high). The shape of the film is modified. Figure 4.3 exaggerates the way the shape of the film might bend under different stress configurations. The motions are small (in the order of $10\ \mu\text{m}$). Therefore, the system is assumed linear. The validation of linearity is presented in Section 4.1.3. The bending stiffness (c_{55}) of this absorber is not taken into account in the simulation since the shear is neglected. The elastic layer is extremely lightweight and resistant to bending. It has the same design as corrugated cardboard.

The DAVA stiffness can be modified in the following manner. The bending stiffness depends on the spatial wavelength and amplitude of the corrugated part. A larger wavelength reduces the bending stiffness in the normal direction. The bending stiffness in the perpendicular direction is extremely high. The design in this case is similar to honeycomb structure. Since this direction was perpendicular to the main direction of the beam on which the DAVA was tested, the added stiffness was not investigated. This stiffness would play an important role on plate type structures. The transversal stiffness of the absorber is locally very small. Globally, it has the same stiffness as a point absorber with similar mass. Thus the DAVA is globally very resistant to crushing although an individual sheet of PVDF is very flexible. The transversal stiffness of the elastic layer can be adjusted using different parameters

- The height of the elastic layer
- The wavelength of the corrugated PVDF
- The thickness of the PVDF sheet
- The electric shunt between the electrodes of the PVDF

Increasing the thickness of the elastic layer will reduce the transversal stiffness. In order to have a device conformal to the structure, this thickness cannot be increased very much. The second parameter that can be modified is the wavelength of the corrugated PVDF. A larger wavelength decreases the transversal stiffness of the elastic layer. This parameter change is also limited. The wavelength should stay small in comparison to the wavelength of the disturbance, otherwise the absorber will lose its distributed properties. The thickness of the PVDF is another parameter that can be changed. A thinner PVDF sheet should lower the stiffness of the elastic layer. The PVDF material used in the prototype is rather thick (110 μ m). Much smaller thickness are available and could be tested.

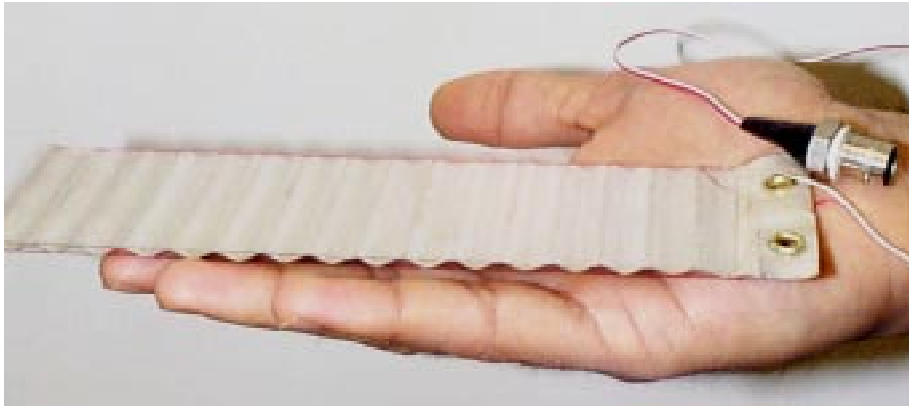


Figure 4.5: Elastic layer with connector.

The last solution to modify the transversal stiffness of the elastic layer is to use the piezoelectric properties of the PVDF. Electric shunts can provide slight changes in stiffness. If an active input is provided to the elastic layer, it can also be controlled to behave “as if” its mechanical stiffness was smaller or larger. Figure 4.5 presents the elastic layer with its electrical wiring connections. The silver-like PVDF can be seen through the transparent plastic sheets positioned on each side of the elastic layer.



Figure 4.6: Prototype #2 distributed absorber with a constant mass distribution

Figure 4.6 is the first DAVA prototype built that was fully functional. The corrugated PVDF can be seen sandwiched between the beam (bottom) and the ??? (top). The DAVA is 2” wide and is glued on a steel beam. It has a constant mass layer made with a 1mm thick sheet of lead. The weight of this absorber is 100g. This type of absorber is not thick compared to the beam. It is conformed to the beam compared to a bulked point absorber such as the one presented figure 2.4.

4.1.2 Manufacturing process

The DAVA requires some precision manufacturing and some patience to build. The main work concerns the construction of the elastic layer. The first step in the making of this layer is to cut a PVDF sheet along its main direction. The DAVA is here intended for a beam. The PVDF has a direction in which the strains will be greater under active excitation. This direction is the main vibration direction of the absorber and base structure. The second step is to remove 1 to 2mm of the silver electrodes on the edge of the PVDF sheet. Acetone is a very good solvent for this matter. The third step is to install a connector linked to each electrode. Figure 4.7 provides a schematic of the connection to a PVDF electrode. Installing this connection is a delicate procedure. At one end of the PVDF strip, two areas are selected to support a rivet. These areas should have an electrode only on one side. One electrode is removed for each area so that the rivets will only be in contact with one electrode. A hole slightly smaller than the diameter of the rivets ($\phi 5\text{mm}$) is cut in these areas. The top of each rivet is soldered to a wire so that it can still be put in place using riveting pliers. An additional piece of plastic can be put on the backside of the PVDF in order to provide a more robust connection. The rivet is then put in place using the riveting pliers. The two wires connected to each electrode can then be soldered to an electrical connector.

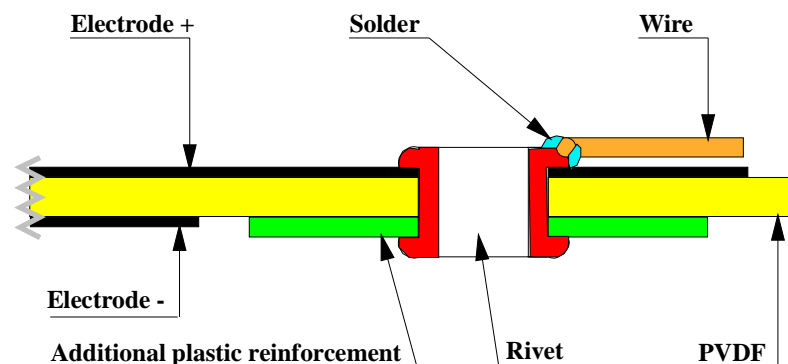


Figure 4.7: Riveted connection to the positive electrode of the PVDF

Figure 4.7 presents a segment view of the rivet on the PVDF sheet with the soldered wire on top of it. The precision with which this connection is built is critical, since very high voltages can drive the PVDF active part of the absorber.

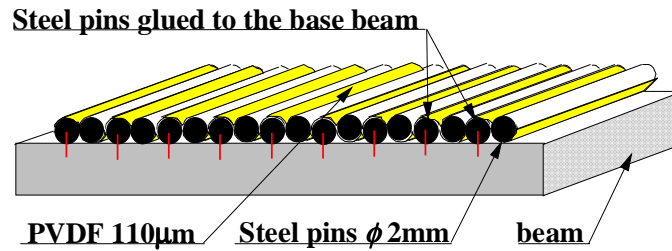


Figure 4.8: PVDF taking its corrugated shape

The next step to build the elastic layer can be performed before the installation of the connections. The PVDF is shaped into its final corrugated form. Calibrated steel pins ($\phi 2\text{mm}$) are glued with epoxy on a beam. The distance between each pin for this prototype was chosen to be 5mm. The PVDF is applied with another set of pins which are positioned in-between the glues ones.

Figure 4.8 presents the setup needed to bring the PVDF into its corrugated form. The PVDF is a plastic material, which needs time to keep its shape and thus has to be kept in-between the pins over several days (3 to 5). For this reason, the additional pins must be kept in place by some artificial mean. Clothes pegs were used for this purpose as can be seen Figure 4.9.



Figure 4.9: PVDF taking its corrugated shape, hold in place with clothes pegs

This particular step is critical. The precision with which the PVDF is placed on the pin and held is important. The uniformity of the waves is determined by the care taken at this stage. There is certainly room for innovation in this process. The method used was adapted for a laboratory experiment and used only common accessories. Bulk manufacturing would require some automation of these steps.

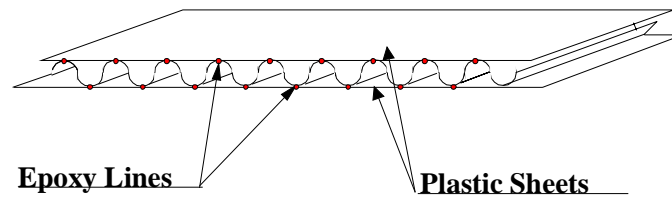


Figure 4.10: Plastic sheets on both side of the corrugated PVDF

The last step in the construction of the elastic layer is to glue the PVDF to two plastic sheets. Note that the plastic sheets were only necessary to improve the ease of hand manufacturing. Figure 4.10 presents the final device built. The glue that was used is epoxy, which has the advantage of drying relatively quickly. The epoxy was deposited in very small amount using hypodermic needles. Fine lines of glue are deposited on top and bottom of each wave of the PVDF. A piece of plastic is then positioned on top of it and maintained in place with a few light weights. The epoxy used dried in five minutes. The other side of the PVDF is then glued to its plastic sheet in a similar manner. The elastic layer is complete at this point.

The mass layer made of sheets of lead can be glued on top of it using cyanocrylate glue. The distributed absorber is also glued on the receiving structure with the same type of glue.

4.1.3 Properties

The absorber can be excited using its active behavior in order to check its dynamic properties. An experiment was developed to validate the active part of the DAVA and at the same time examine its absorber resonant behavior.

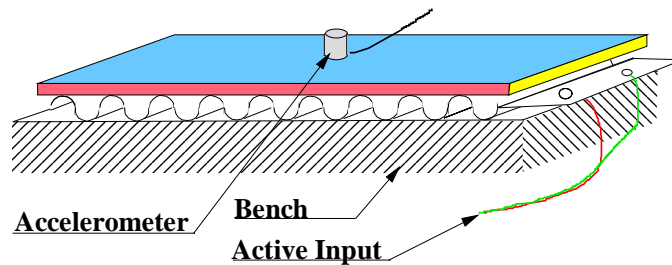


Figure 4.11: Experimental setup for validation of active behavior

Figure 4.11 presents the experimental setup. The base of the absorber is “clamped” since it is glued to a heavy bench. On top of the absorber, an accelerometer measures the mass vibration. The active input is white noise at $100V_{\text{rms}}$. Figure 4.12 presents the frequency response of the mass layer in respect to the active input. The measurements were taken from 100 to 1600Hz.

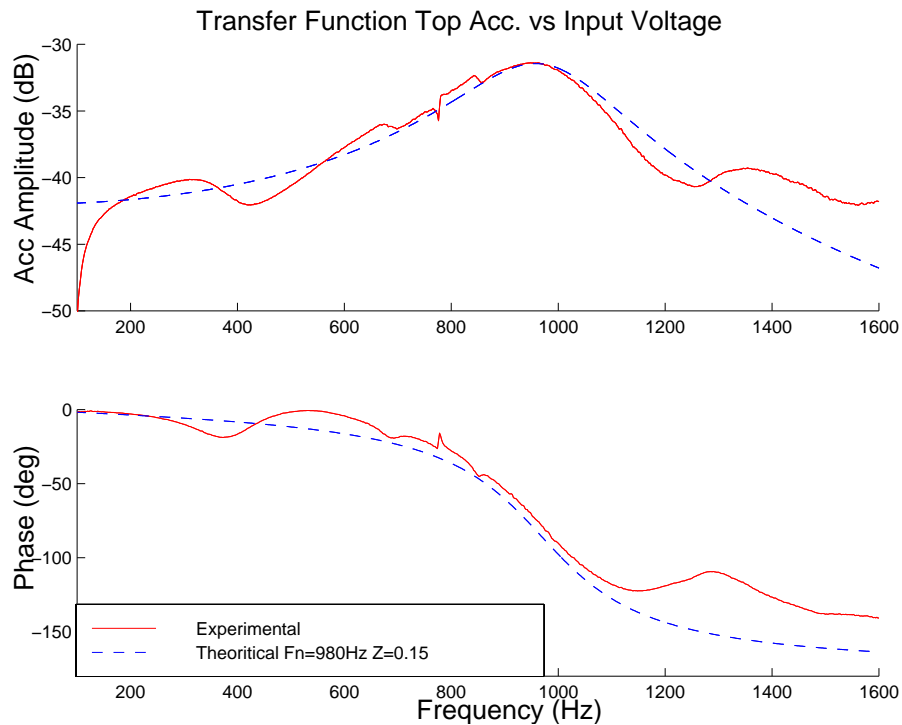


Figure 4.12: Frequency response of a self-excited distributed absorber

The response is typical of a heavily damped absorber. It shows a peak in acceleration amplitude and a 180° phase shift. The behavior of the distributed absorber is similar to a single degree of freedom model. However, the DAVA used in this experiment is not a perfect one degree of freedom system. It appears from Figure 4.12 that at around 1300Hz another resonance starts. This type of imperfection is due to the manufacturing of the elastic layer. For example, some part of the absorber might be stiffer than some other part. The resonance frequency of the absorber is not unique all over the area of the DAVA and the transfer function looks slightly different than for the classical point absorber.

The linearity of the distributed absorber was checked using the same setup of figure 4.11. The absorber is excited at a single frequency near its resonance frequency (1000 Hz) in order to maximize the displacements. The voltage used was 200 V. Figure 4.13 presents the autospectrum of the signal from the accelerometer. An ideally linear device should have around a 60 dB reduction between the fundamental and the first harmonic. For the distributed absorber, the first harmonic is more than 30dB below the fundamental. On an

oscilloscope, the accelerometer signal looks like a perfect sinusoid. Even if this is not ideal, the distributed absorber can be thus considered as a linear device.

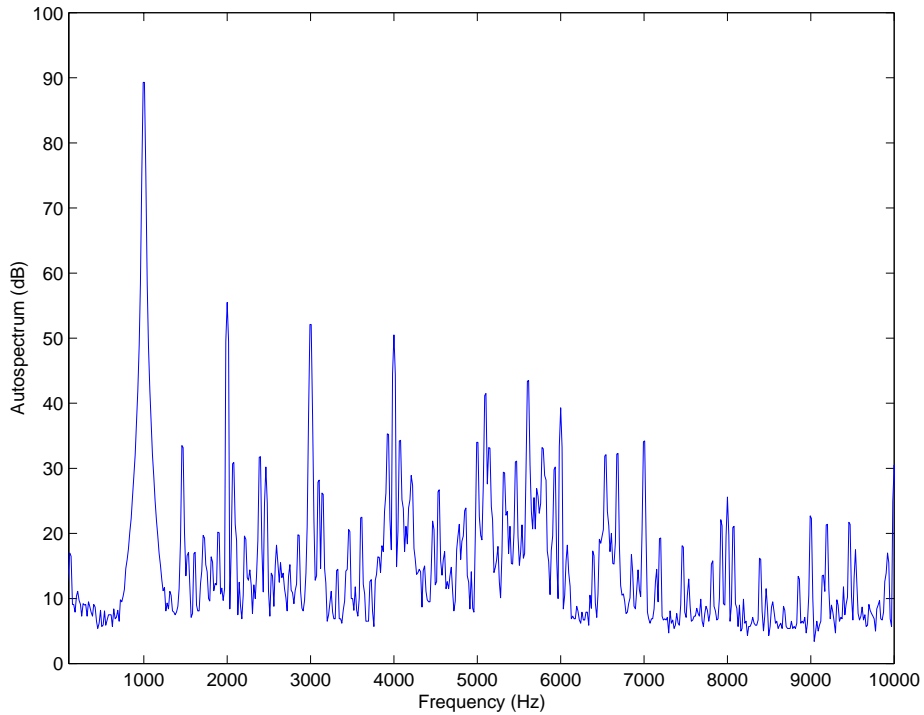


Figure 4.13: Harmonics for a self-excited distributed absorber at 1000Hz

The design presented in this subsection is suited to a particular structure used for experimental validations. This structure is a beam, which is very thick and heavy compared to elements used for example in the aerospace industry. The main reason was to have an absorber easily manufactured with non-precision tools. Using a quality manufacturing process, thinner PVDF film and thinner mass layers may improve the performance of the absorber and, in the same time, reduce its size and resonant frequency.

4.1.3 Experiment with passive absorbers and theoretical comparison

The experiments were performed on a simply supported beam. The properties for the beam can be found in Table 3.I. The beam was positioned on a heavy bench (20 Kg) with perpendicular thin sheets of aluminum for the approximation of simply supported boundary conditions. The excitation was performed using anti-symmetric (on each side of the beam) piezoelectric patches. Wood baffles arranged in the plane of the beam allowed the measurement of radiated sound in an anechoic chamber and comparison with the analytical model of Appendix A. Reflective tape was added to the beam in order to measure normal beam velocities with a laser velocimeter.



Figure 4.14: Experimental beam setup with baffles

Figure 4.14 is a picture of the beam positioned in the wood baffle. The main length of the beam is 61cm (24"). The distributed absorber was positioned on the other side of the beam as can be seen Figure 4.15. The absorber covers $1/4^{\text{th}}$ of the length of the beam and it is placed next to one end, covering half the wavelength of the 4^{th} beam mode.

The behavior of the distributed absorber was compared to the point absorber shown Figure 2.4. The point absorber was positioned in the center of the area taken by the

distributed absorber (without the DAVA in place). The weight of each type of absorber is 100g, which represents only 4% of the beam weight. The experimental measurements and simulations were performed for this same setup.

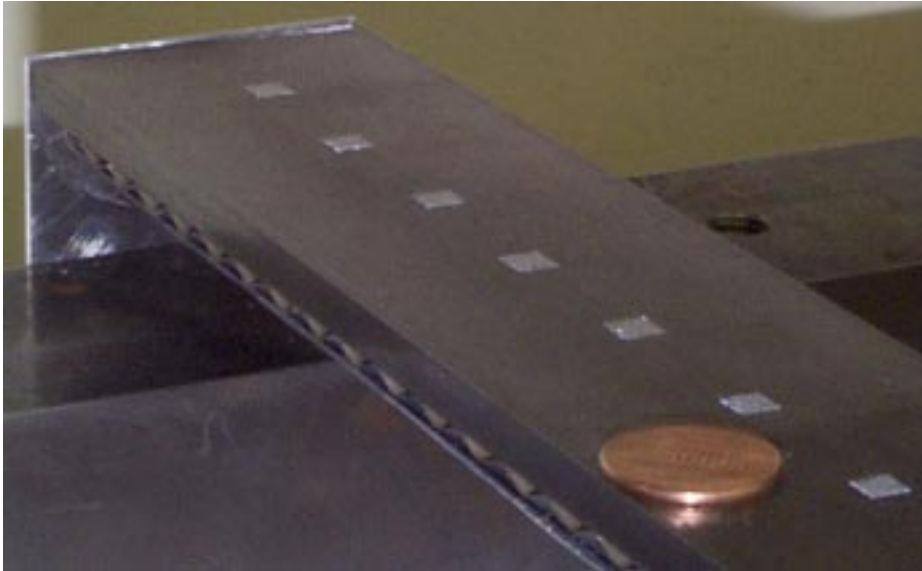


Figure 4.15: End of the beam without the baffles

The corrugated PVDF of the DAVA can be seen on Figure 4.15. A one cent coin gives the scale of the picture. On the same figure, the aluminum sheet used for the simply supported boundary condition can be seen at the end of the beam.

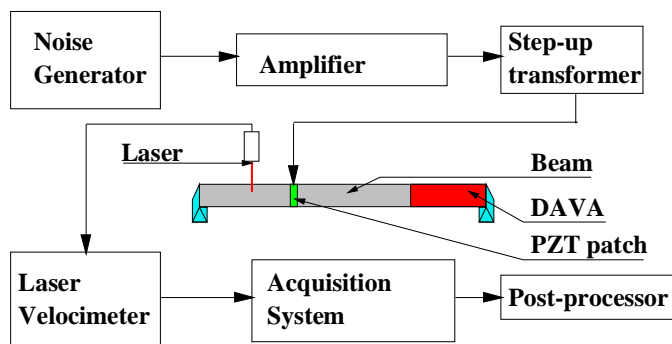


Figure 4.16: Experimental setup for testing the DAVA

Figure 4.16 presents the experimental setup used to measure the performance of the DAVA compared to a point absorber. This same experiment is also aimed at tuning and validating the simulation. A noise generator provides a white signal of frequency band [0 to 1600Hz]. This signal is then amplified and passed through a voltage step-up transformer (the PZT needs high voltage with low current [6]). The output of the transformer is used to drive the PZT that then actuates the simply supported beam shown Figure 4.14. A laser velocimeter measures the normal velocity along the beam. Its output is acquired by a data acquisition system (PC + acquisition card + associated software). A personal computer is then used to post-process the data. From this data, the results of Figure 4.17 is obtained. This figure presents the mean square velocity of the beam. This data can be associated to the average kinetic energy of the beam. It is computed by summing the squared velocities of every point and by dividing by the number of points (23). The mean square velocity is normalized per volt of excitation. It is presented from 100Hz to 1600Hz. This frequency band does not include the first mode of the beam, which is at 40Hz. The blue line presents the measurement of the beam alone. The second to the sixth mode of the beam can be observed in order. The green line presents the behavior of the beam with the 100g point absorber. The resonance frequency of this absorber is 850Hz. The absorber will therefore have an effect on the fifth mode. This mode is split in two resonances with smaller peak values. With a better tuning (resonance frequency of the absorber at 1000Hz) these peaks would be slightly moved to the right of the axis and centered around 1000Hz.

The red line presents the behavior of the beam with the DAVA. In this experiment, the DAVA is used as a passive device. The attenuation provided by the distributed absorber can be seen to be different from the point absorber. At exactly 1000Hz the performance is not as good as a perfectly tuned absorber (cf. simulation Figure 4.18). The distributed absorber does not split the fifth mode and the peak value is much smaller than the peaks appearing with the use of a point absorber. However, some significant reduction is also achieved for the third, fourth and sixth mode. Note that the point absorber achieves very small reduction in comparison. The yellow line refers to the beam with the mass layer of

the DAVA directly glued to it. The added mass result demonstrates only slightly changes the resonance frequencies and adds only a little damping. This that the DAVA works by using a dynamic effect (reactive force) to control the beam vibration similar in concept to the point absorber. Figure 4.11 presents the same setup, this time simulated by the model described in Chapter 3. This time, the point absorber is tuned exactly to 1000Hz (this is the power of the simulation). The global behavior for each test case matches the experiment well. This simulation validates in particular, the distributed absorber model.

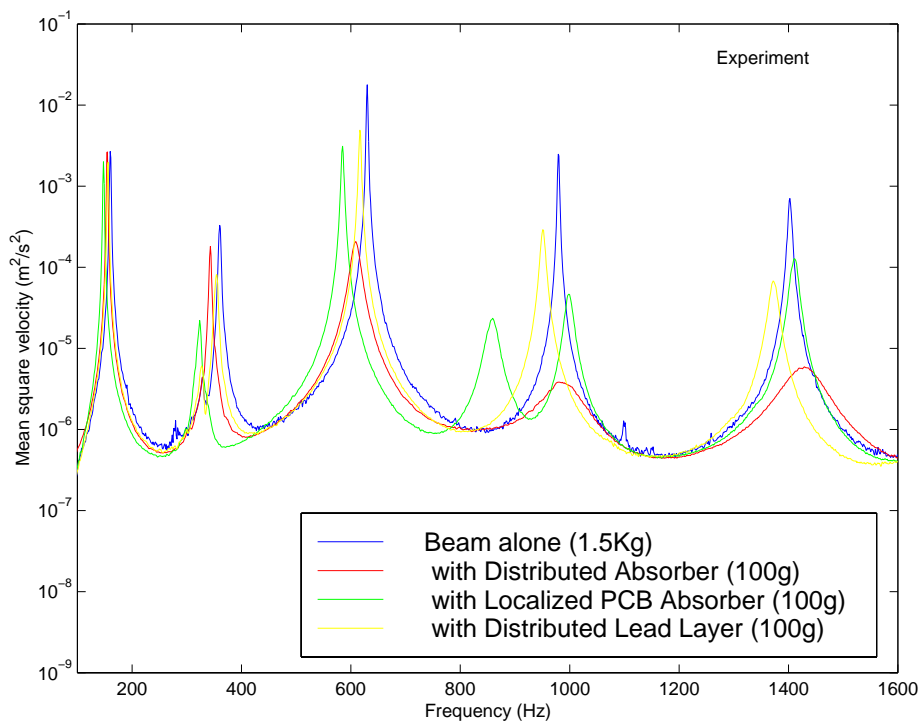


Figure 4.17: Beam with a 6" distributed absorber

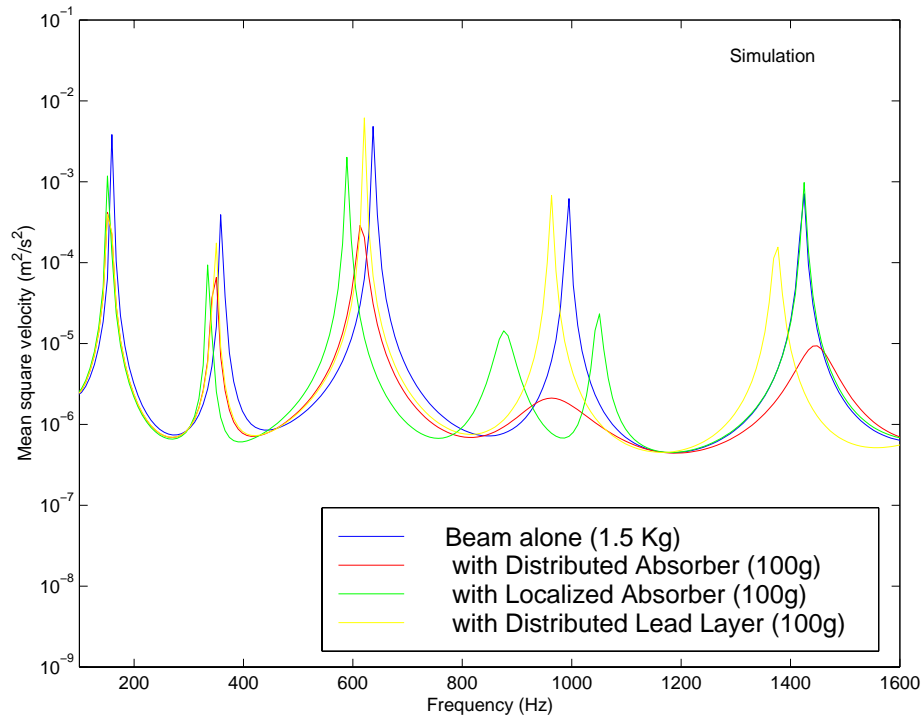


Figure 4.18: Simulation of the same setup

The simulation shows even more clearly the difference between the two types of absorber. The point absorber is very efficient at reducing the response at a single frequency. The energy is just moved to different frequency bands and two new resonance are created. The distributed absorber does not have this drawback. The vibration energy of the beam is diminished for all the resonance frequencies of the beam and no new resonance appears. The distributed absorber is potentially able to control several modes at a time at different frequencies. This property might be extremely useful for the damping of modally dense structures such as plates. The simulation model is an extremely valuable tool. It will be used to improve the design of the distributed absorber, as discussed be demonstrated in Section 4.2.

4.1.4 Experiment with active absorber

An active control experiment was then performed using the same prototype of the distributed absorber (several version of this absorber have been assembled). The control

system employed 3 accelerometers as error sensors, pass-band filters, and a feedforward LMS controller (implemented on a C40 DSP board) [6].

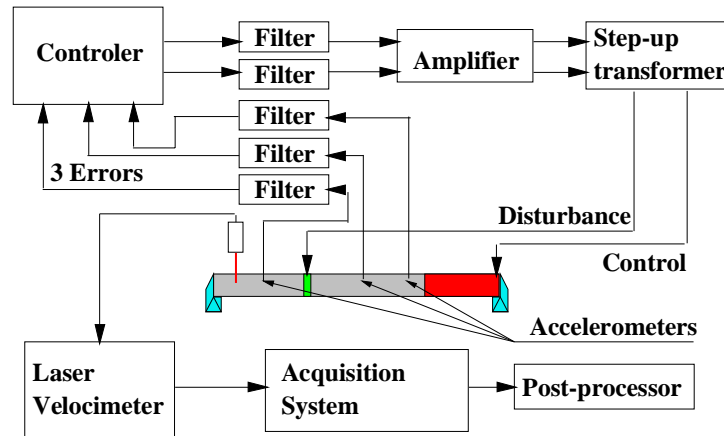


Figure 4.19: Experimental setup for active control experiment

The experimental setup presented figure 4.19 is in part similar to figure 4.16. The vibration measurements are again done with the laser vibrometer. The disturbance is again white noise generated by the same DSP used to implement the controller. The controller attempts to minimize the error sensor signals by controlling the beam with the active part of the DAVA. All the inputs and outputs of the controller are filtered with band pass filters. The control algorithm used is called the LMS algorithm [6]. This algorithm optimizes a set of N adaptive filters in order to minimize an error signal knowing a set of inputs. The algorithm can be used to model a linear system. Such system is a linear combination of its past inputs (digital signals are implied). A gradient method is used to find the optimum weight to be associated with the N past values of the system inputs. The error signal used for the gradient search is the difference between the real output of the system and the output of the adaptive filter.

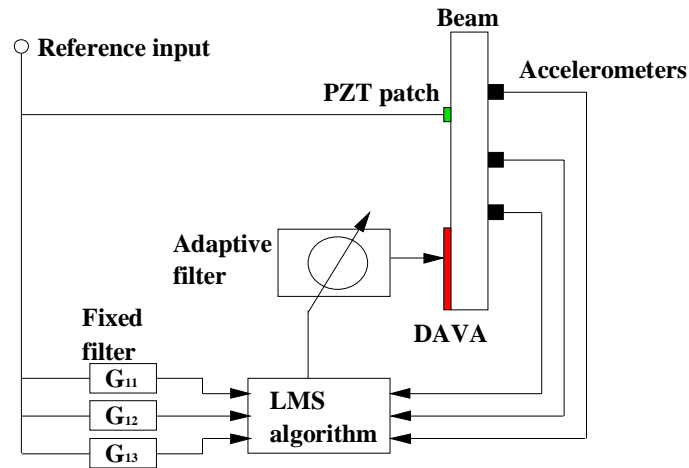


Figure 4.20: Schematic layout of controller and test rig

Figure 4.20 presents the control loop. In this experiment, the disturbance signal is also used as the reference signal. This reference signal has to be filtered by estimate of the transfer function between the DAVA and each error sensor (accelerometers).[6] These transfer functions are obtained by system identification using the LMS algorithm. The LMS algorithm optimizes the gains of the adaptive filter in order to minimize the error signals.[6]

The controller software used by the DSP was developed at the VAL group in Virginia Tech. The control loop minimizes the vibration at the error sensor locations using the active input on the distributed absorber (DAVA). The different parameters for this active control experiment are presented in Table 4.II.

Table 4.I: Parameters for active control

Error sensors	3
Active absorber	1
Disturbance	PZT patch
Reference	Internal
Sampling frequency	5000 Hz
System ID filter coefficients	120
Control path filter coefficients	180

The error sensors were respectively positioned at $-7.5''$, $-1.5''$, and $5.5''$ from the center of the beam. Vibration measurements were performed using the laser velocimeter every inch

of the beam (23 points overall). The mean square velocity of the beam has been computed and is presented Figure 4.21.

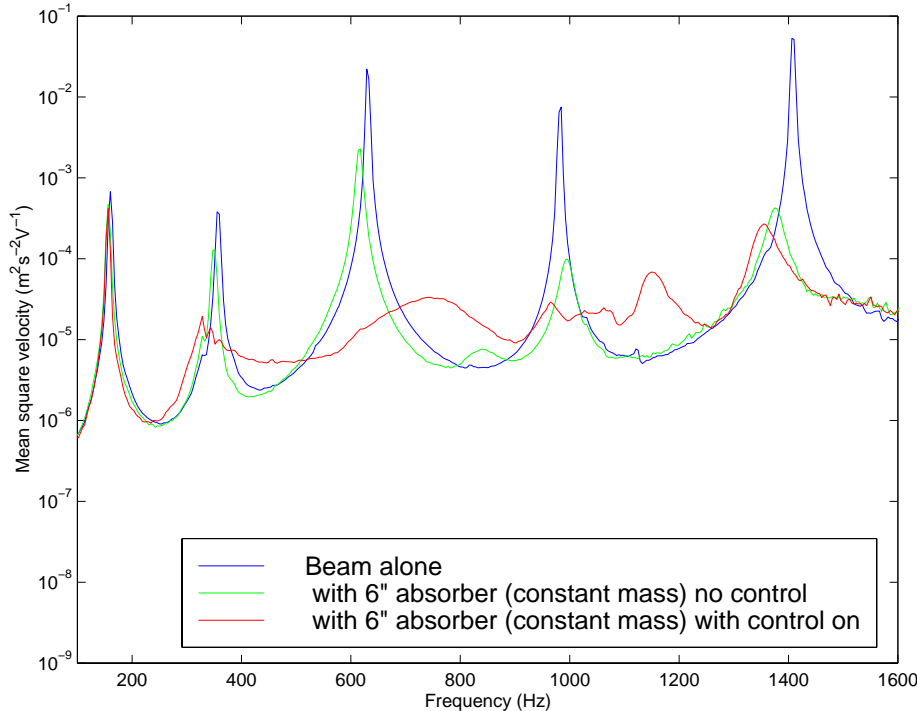


Figure 4.21: Active control experiment with distributed absorber (constant mass distribution)

The green line presents is the behavior of the beam with the DAVA acting as a passive device. The reduction in mean square velocity obtained in this passive configuration is 10dB for the frequency band [100 1600Hz]. This result is similar to the trends presented in 4.1.3. With the active control on, Figure 4.21 demonstrates that an additional 3dB is obtained. The behavior of the beam controlled actively by the DAVA is presented by the red line. The performance of the active system is very good at reducing the resonance peaks. A 20dB reduction is for example obtained at 600Hz, which was the most important peak before control. In between resonances, the active control increases the vibration (termed control spillover). A better controller and more error sensors should reduce this problem. With the active control on, the structure has a non-resonant behavior. The absorber adds a significant damping to the system, which makes the active control more difficult (the system response becomes less predictable). No active control

is obtained below 400 Hz due to the poor response of the PVDF and of the absorber itself (cf. Figure 4.7). It appears that in order to increase the efficiency of the absorber, the mass distribution needs to be optimized. A typical beam response has varying amplitude and phase (dynamics) along the beam and the result can be thought of a sum of many SDOF systems. This suggests that instead of keeping the mass distribution constant, the next prototype should have a varying mass layer all along the beam. The varying mass distribution will alter the local properties of the DAVA to ideally match the locally varying response properties of the base structure.

4.2 Distributed absorber with optimal mass distribution

4.2.1 Optimization

The experiments presented in 4.1 were developed to validate the properties of the active-passive distributed absorber. As discussed in the previous section an enhanced version of this absorber would be fully distributed and have a varying mass distribution since the beam/DAVA response is complicated along the beam it is necessary to derive an optimal process for choosing the mass distribution. The genetic algorithm was chosen to provide a good solution to this problem. This algorithm has been described in Chapter 2. The parameters used for the optimization process are provided in table 4.II. For these example results the distributed absorber was optimized to minimize the total radiated power of the beam when active control is on over a frequency band of 800 to 1200Hz. Other performance goals could be chosen if needed.

Table 4.II: Optimization with a genetic algorithm

Starting generation	10 first P_{sin_r}
Number of generation	46
Number of individual per generation	10
Number of bit per chromosome	45
Fitness	$1/(\text{Radiated Power})$
Rate of mutation	0.03

For the optimization task the total mass of the layer was kept constant (100g) and its thickness varied. The mass redistribution obtained with the genetic algorithm is certainly not necessarily the best possible one. The example solution is a mass distribution from a set of possible solutions that performs well.

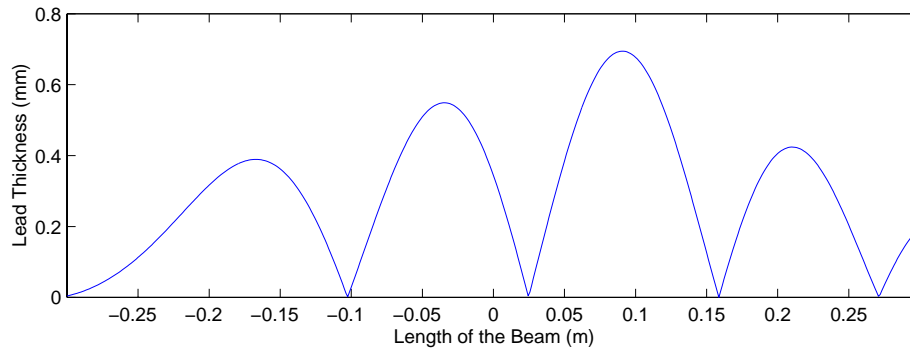


Figure 4.22: Mass distribution optimized for the radiated power [800 1200Hz]

Figure 4.22 present the mass distribution of the absorber. This mass distribution is in fact the absolute value of a optimization objective function that may be negative. In the particular distribution of Figure 4.22, each alternate lobe is negative. A part of the DAVA with a “negative mass” means that the motion is in the other direction (180 degree out-of-phase) compared to the parts with “positive mass”. For this reason the parts associated with a “negative mass” are wired in opposition to the ones with “positive mass”. The mass distribution is described with the nine first Psin functions and the coefficients associated with each of these functions are presented in table 4.III.

Table 4.III: Coefficients for the mass distribution

Order of Psin function	1	2	3	4	5	6	7	8	9
Coefficient	0	0.2	0.333	0.8	0.333	0.067	0.067	0.933	-0.6

The number of function used is very small. More functions may give a better solution. The advantage of having few coefficients is that the distribution will be relatively simple and therefore easily manufactured.

4.2.2 Experimental investigation

The prototype was build using the same techniques has in section 4.1. The absorber is divided in four sections. Each section DAVA is wired with the opposite phase of its neighbors for the reasons discussed above. Several thin sheets of lead (0.1mm) stacked

on top of each other are used to approximate the optimal mass distribution curve of Figure 4.22.

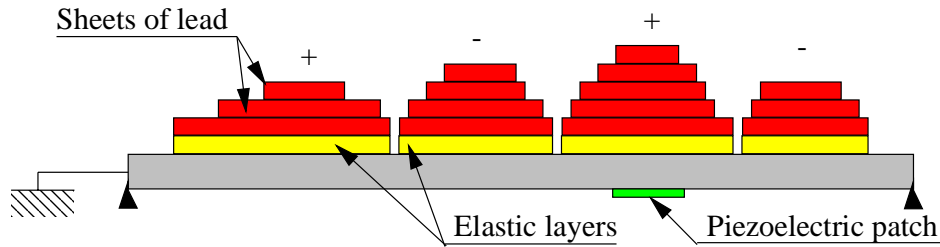


Figure 4.23: Discretized mass for the distributed absorber, prototype #3

Figure 4.23 schematically shows the configuration of the DAVA with optimally varying mass distribution. The sign on top of each part of the absorber refers to the polarity of the elastic PVDF sheet in respect to the piezoelectric drive patch (the disturbance). (It is interesting to notice that the disturbance (piezoelectric patch) is located where the absorber has the more mass. The beam response used in the optimization procedure is strongly dependent upon the disturbance location. It appears that the maximum reactive dynamic effect of the DAVA occurs in direct opposition to the disturbance which is logical.)

The beam is grounded and the PVDF ensured not be in contact with the beam in order to avoid short-circuits. The plastic sheet on the down side of the absorber is useful for this purpose and is used electrically to isolate the PVDF from the beam. The distributed absorber is glued on the underside of the beam using cyanocrylate glue.

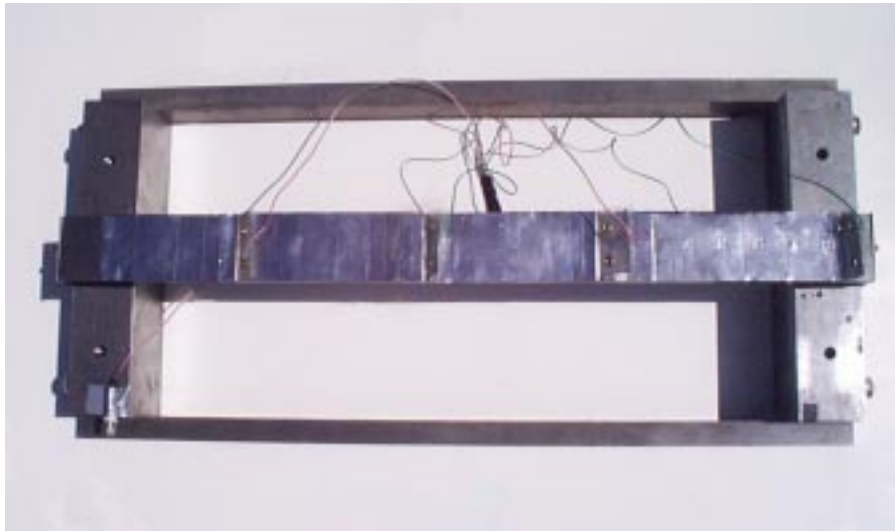


Figure 4.24: Distributed absorber with optimal mass distribution

Figure 4.24 is a picture of the beam turned to show its underside with the distributed absorber. The four parts of the absorber are connected to a single connector. It is thus considered as a single actuator. The active control setup and parameters are similar to the ones presented in Table 4.I. Note that experimental controller is designed to minimize vibration at three accelerometer locations as before and not radiated power as in the optimization process. This was chosen as it was very difficult to measure radiated pressure as the signals were very low. However radiation is directly tied to the beam response and thus the experimental results are likely to be satisfactory (as will be seen). An improved experiment would utilize a very wide beam (a 1-D plate) with higher radiated sound levels thus improving the SNR of the error signals. Figure 4.25 presents the same type of data as Figure 4.21. These two figures are intended for the comparison between a DAVA with a constant mass distribution and a DAVA with optimal mass distribution. The distributed absorber with an optimal mass distribution is seen to perform better than one with constant mass. As a passive device (no control), a 13dB reduction is obtained for the frequency band [100 1600Hz]. With the active control on, the results are significantly better. An additional 6dB reduction is obtained over the same frequency band. The control is still not efficient under 400Hz and above 1400Hz. The reason is that the distributed absorber does not have much active control authority on the beam at

frequencies far from its main resonance and was optimized for the 800 to 1200Hz band. The shape of the distributed absorber and its lowest resonance frequency, which is around 1200Hz, limits its active actuation ability at low frequencies.

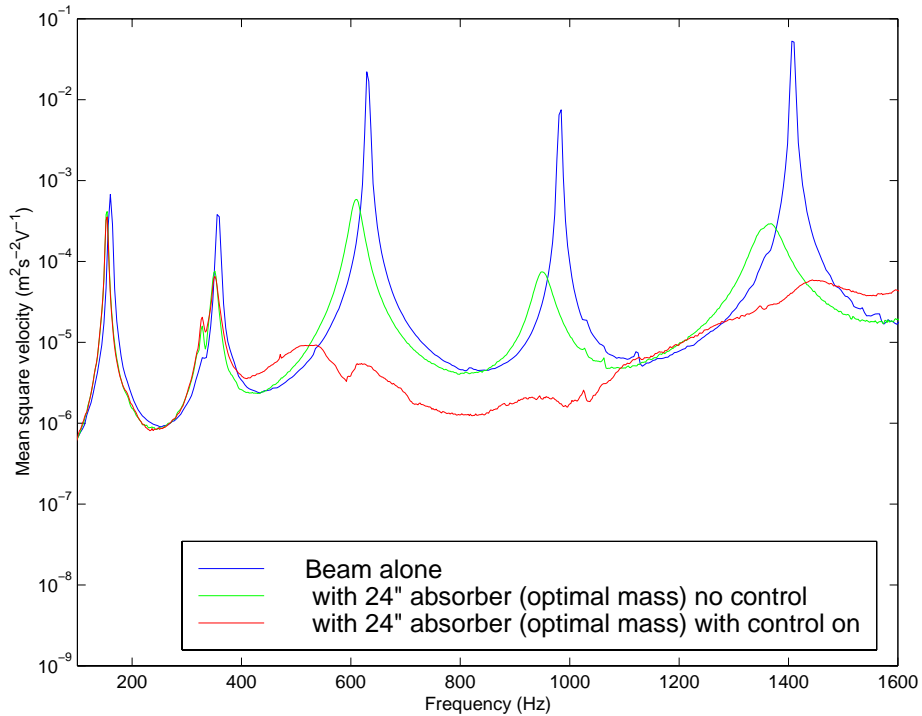


Figure 4.25: Active control experiment with distributed absorber (optimal mass)

However the very good active performance of the distributed absorber with optimal mass distribution validates the genetic search. It also demonstrates the power of the simulation and the optimization tool to enhance the particular design.

Table 4.IV: Summary of the vibration reductions obtained experimentally (dB) for frequency band [100 1600]Hz

24" Constrained layer	7
6" Distributed absorber with constant mass distribution	10
6" Distributed absorber with constant mass distribution with active control on	13
24" Distributed absorber with optimal mass distribution	13
24" Distributed absorber with optimal mass distribution with active control on	19

Table 4.IV summarizes the reduction obtained with the different devices investigated. The first remark is that the mass distribution can be seen to be a critical part of the distributed absorber and needs to be optimized. The classical approach that takes only into account the resonance frequency of the absorber for the tuning is not appropriate in this case. A thinner mass layer distributed along the beam is more efficient than a thick one covering $\frac{1}{4}$ of the length. The second reason in distributing and optimizing the mass is the active control performance. An optimal mass distribution can significantly reduce the vibration level (6dB) with active control on. The second remark concerns the efficiency of the active control. With an optimal mass distribution, the active control improves significantly the performance of the DAVA. The increased difficulty of implementing an active-passive system in place of purely passive system can be justified in this case.

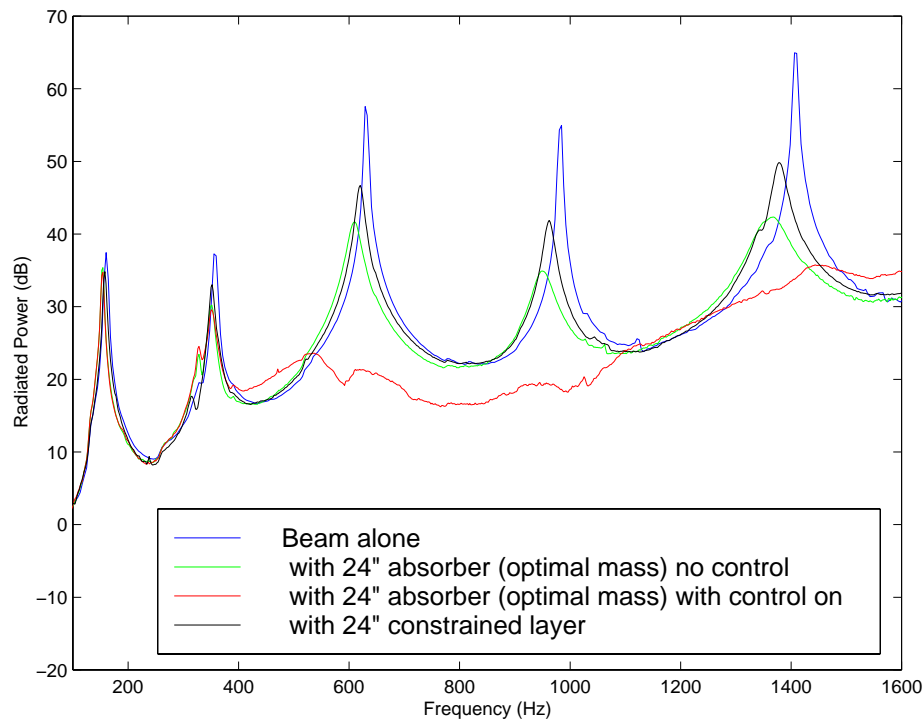


Figure 4.26: Beam with distributed absorber (optimal mass) and constrained layer

The mass distribution was numerically optimized for the sound radiation. The structured error sensors can be understood as filtered sensors for the radiated power. Even if the

relationship is extremely complex between the acceleration of the three points of the beam and the radiated power, this relation exists. In this particular case it seems that this relationship was favorable. Controlling the three structural points actually reduced the radiated power of the beam. Figure 4.26 presents the radiated power of the beam between 100Hz and 1600Hz.. The sound radiated power is computed from the vibration data using the relations of Appendix A since the beam does not emit enough sound to be measured in an anechoic chamber. The absorber can be seen to perform very well in reducing the radiated power of the beam for the frequency band it was designed: [800 1200Hz]. The radiated power is also reduced dramatically at the 600 and 1450 Hz resonance peaks. This performance is particular to this experiment since the errors sensors were not designed to reduce the radiated power but the vibration of three points of the beam. However it still demonstrates the use of the DAVA for reducing sound instead of vibration.

One important final question is “How does the DAVA perform compared to a traditional distributed vibration treatment such as a constrained layer damping material?” For this purpose an experiment was run using constrained layer damping material alone. Another data set is added on Figure 4.26 concerning a constrained layer. The constrained layer is produced by Polymer Technologies, Inc. The characteristics of this constrained layer can be seen in Table 4.V. The weight was chosen to be identical to the DAVA.

Table 4.V: Constrained layer damping properties

Length	24"
Weight	100g
Thickness of viscoelastic layer	1mm x 2
Thickness of aluminum layer	0.5mm

Constrained layer damping are a very common damping treatment. This comparison is a good way to evaluate the overall performance of the active-passive distributed absorber. The results, shown also in Figure 4.26, demonstrate that the absorber is more efficient than the constrained layer in reducing the resonance behavior of the beam for the considered frequency band. The constrained layer has the advantage of being efficient on

a very large bandwidth and especially at high frequency. The distributed absorber can be targeted at a smaller bandwidth but is more efficient in this chosen bandwidth especially with the active control on. The DAVA concept is therefore competitive compared to the conventional (and more simple) constrained layer damping treatment.

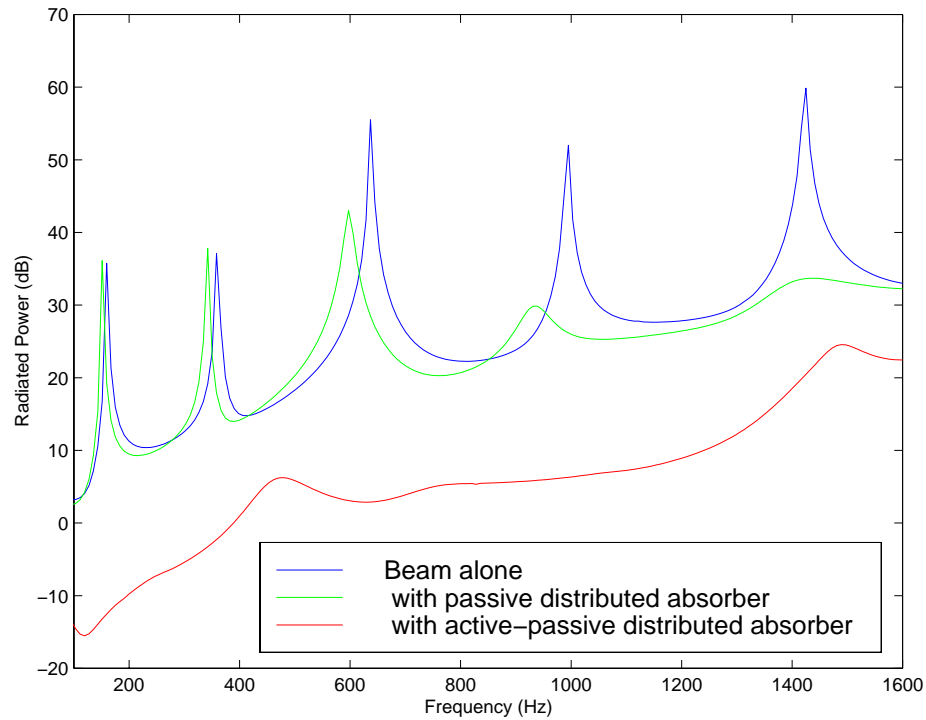


Figure 4.27: Simulation of the best possible control

Figure 4.27 present the simulation of the experimental setup. The red line is the best possible active control solution. No limitation on the control voltage is imposed. The simulation can be seen to be reasonably similar to the experimental data of Figure 4.26. The behavior of the absorber with no control is well modeled except for the peak at 1450 Hz. The reason is that the absorber is not perfectly built. The corrugated PVDF is not perfectly even and some of the waves are not perfectly bonded to the upper or lower plastic sheets. These imperfections are certainly critical at high frequency. A large part of the predicted control is achieved experimentally but there is still room for improvement. One main reason for the difference lies in the dynamic range limitations of the control DSP used in the experiments (approx. 30dB). It is interesting to notice that the

experimental curve and the simulated are almost parallel. The control can be considered as relatively efficient. The vibration of the three points on the beam is remotely linked to the radiated power of the beam. Thus another reason for the discrepancy is that only part of the alternation is achieved. The experiment is still very impressive in term of reduction performance when compared to the simulation. The ability of a distributed active vibration absorber to reduce sound and vibration has been unequivocally demonstrated.